



71st Conference of the Italian Thermal Machines Engineering Association, ATI2016, 14-16
September 2016, Turin, Italy

Internal power recovery systems for cryogenic cooling plants: secondary compressor development

A. Giovannelli*, E. M. Archilei, E. Palazzo

Dept. of Engineering, Roma Tre University, Via della Vasca Navale, 79, Rome, 00146

Abstract

Refrigeration systems consume a relevant amount of electrical power worldwide. For this reason, in the last decades, several energy saving techniques have been proposed to reduce the power demand of such plants.

The present paper deals with the development of an innovative internal power recovery system for industrial cryogenic cooling plants. Such an innovative system consists in a Compressor-Expander Group (CEG) for internal power recovery. In particular, the paper is focused on the development of the CEG compressor, which has to pre-compress the refrigerant main flow before the fluid enters the main compressor. The machine has been re-designed, modifying a centrifugal compressor for automotive turbocharging. To verify the performance and suggest improvements, a numerical fluid dynamic model has been set up and the commercial Ansys-CFX software has been utilized to perform steady-state 3D simulations.

Expected performance of the secondary compressor are presented and discussed in this paper.

© 2016 The Authors. Published by Elsevier Ltd. This is an open access article under the CC BY-NC-ND license (<http://creativecommons.org/licenses/by-nc-nd/4.0/>).

Peer-review under responsibility of the Scientific Committee of ATI 2016.

Keywords: Centrifugal Compressor; Energy Saving; Organic Fluids; Refrigeration Plants; Vapor Compression Systems

1. Introduction

Recently, many improvements have been proposed to Vapor Compression Refrigeration (VCR) plants. Some of them aim for the reduction of electrical power consumption at constant cooling power, while other solutions bring to an increase of the system cooling power at constant plant consumption. Multi-stage compressions, the utilization of a liquid sub-cooling exiting the condenser, internal recoveries in the system are the most relevant ones. [1].

* Corresponding author. Tel.: +39 06 57333424; fax: +30 06 5593732.
E-mail address: ambra.giovannelli@uniroma3.it

Nomenclature

CEG	Compressor-Expander Group
COP	Coefficient of Performance
D	reference diameter
F	Cooling Power
h_0	total specific enthalpy
M_{b1}	optimized first bleed flow
M_{b2}	optimized second bleed flow
M_{c1}	optimized auxiliary compressor flow
N	rotational speed
P_c	main compressor power demand
p_0	total pressure
R	specific gas constant
Re	Reynolds number
T_0	total temperature
V	volumetric flow
VCR	Vapor Compressor Refrigeration
γ	ratio of specific heats
η	efficiency
ρ	density

The present work deals with the development of a device for internal power recovery in large VCR plants. Such a device is based on Ascani's patent [2], an interesting proposal that requires minor plant modifications and could be applied in new cryogenic plants as well as for the upgrading of traditional ones.

The plant concept is depicted in Figure 1a. The common basic VCR scheme is modified adding two extractions at the condenser exit. The extracted flows are expanded and heated by means of valves (components 22 and 24) and recovery heat exchangers (23 and 25). Then, they complete their expansion in two auxiliary expanders (28 and 29) before entering the Main Compressor (20). The main flow, sub-cooled in the recovery heat exchangers, passes through the main expansion valve (26) and the evaporator (27). Then, it is sent and pre-compressed into an auxiliary compressor (30). Such a compressor is connected and moved by the auxiliary expanders. All the flows expanded or pre-compressed in the recovery system (11, 15 and 19) are mixed together before entering the Main Compressor.

By means of such recovery system, improvements in plant performance are expected.

2. Reference Plant

On the basis of Ascani's concept, a 100 kWc cryogenic plant was analyzed and optimized. The system optimization process is widely described in [3]. For the development of the CEG prototype, a simplified plant layout not far from the original one proposed by Ascani, was taken into consideration. In Figure 1b the scheme is shown. Both the liquid extractions after the condenser have been maintained, but only one of these is utilized for mechanical power production in the recovery system. The auxiliary expander moves the secondary compressor, which pre-compresses the flow exiting the evaporator, reducing the main compressor power demand. The liquid extracted with the second bleed, after the pre-heating, goes directly into the main flow entering the Main Compressor.

Table 1 summarizes the comparison of the global performance quantities between the traditional cycle (A) and the new configuration (B) depicted in figure 1b. Moreover, table I reports the bleed flows (M_{b1} and M_{b2}) and the secondary compressor mass flow (M_{c1}) achieved by means of the optimization process [3]. Such results are relevant as starting point for the preliminary design of CEG components.

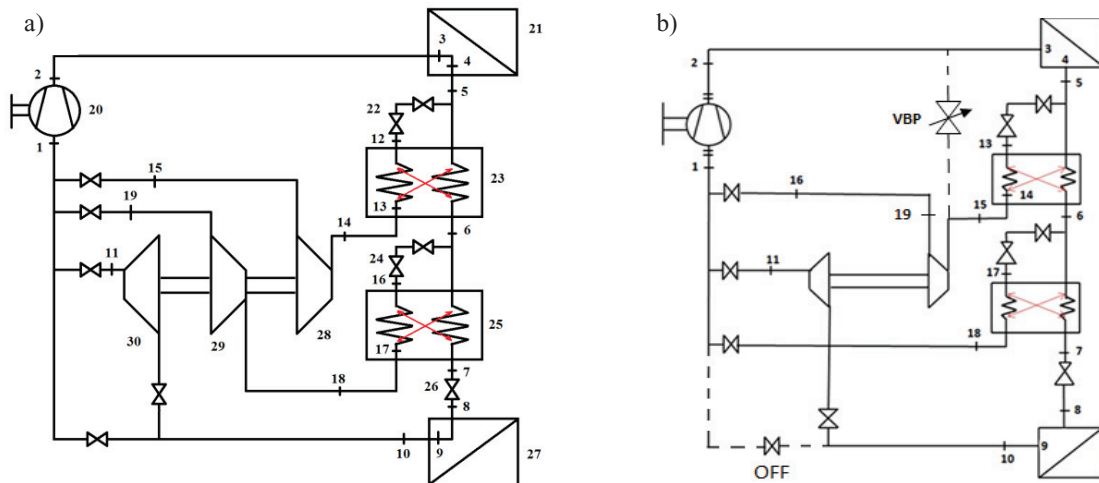


Fig. 1. (a) VCR system proposed by Ascani; (b) VCR layout with a single internal recovery

Table 1. Comparison between 100 kW simple VCR cycle and optimized cycle with internal recovery

	Simple Cycle (A)	Cycle with internal regeneration (B)	(B-A)/B [%]
F [kW]	100.00	100.00	0
Pc [kW]	101.50	74.98	-26
COP	0.98	1.33	36
Δh_{ce} [kJ/kg]	84.18	178.20	112
Mmc [kg/s]	1.19	1.05	-12
Mb1 [kg/s]		0.31	
Mc1 [kg/s]		0.56	
Mb2 [kg/s]		0.18	

The optimization process has been carried out at constant evaporation and condensation temperatures ($-40\text{ }^{\circ}\text{C}$ and $+40\text{ }^{\circ}\text{C}$, respectively). Moreover, constant sub-cooling and over-heating effects ($\Delta T_{sc} = \Delta T_{sh} = 5\text{ }^{\circ}\text{C}$) have been taken into account. All the evaluations have been carried on taking R404a into consideration as reference refrigerant working fluid. Comparing performance of the optimized VCR with a single internal recovery and performance of the basic VCR system, it is possible to highlight a relevant decrease in the system power demand P_c (-26%) that leads to an increase of the Coefficient Of Performance (COP) of about 36%. Such a coefficient is a global quantity which, usually, summarizes VCR plant performance and it is defined as the ratio between the cooling power F and the power required by the main compressor P_c .

3. CEG Machinery Selection

At the beginning, both positive displacement machines and turbomachines have been taken into consideration for the design of the CEG system. Finally, machines from automotive turbocharging technology have been chosen, on the basis of compactness, availability, reliability, high performance and low cost considerations.

Similarity rules have been applied for the preliminary selection of reference machines, both for the CEG secondary compressor and expander [4, 5]. It is well known that turbomachine performance can be correlated to a certain number

of independent variables. In a non-dimensional form the pressure ratio (p_{0out}/p_{0in}) and the efficiency η can be expressed as function of four non-dimensional independent groups [6, 7]. In [6] the relationship is expressed as:

$$\frac{p_{0out}}{p_{0in}}, \eta = f\left(\frac{\rho V \sqrt{\gamma R T_{0in}}}{D^2 p_{0in}}, \frac{ND}{\sqrt{\gamma R T_{0in}}}, Re, \gamma\right) \quad (1)$$

being the first non-dimensional group the flow capacity and the second one the blade Mach number. If the Mach number is preserved and the Reynolds number (Re) is sufficiently high, the relationship (1) can be simplified and just two non-dimensional groups are necessary for the description on the turbomachine performance. Moreover, as reported in [3], having sufficient information for technologies commercially available, it is possible to correlate performance with such non-dimensional groups. Therefore, the relationship (1) can be simplified and re-arranged as follows:

$$\frac{p_{0out}}{p_{0in}}, \eta = f\left(\frac{NV^{\frac{1}{2}}}{\Delta h_0^{\frac{3}{4}}}, \frac{D\Delta h_0^{\frac{1}{4}}}{V^{\frac{1}{2}}}\right) \quad (2)$$

being the first non-dimensional group connected with the machine speed and the second one with the geometry.

Such information was implemented in the tool developed for the cycle optimization. In such a way, once the cycle layout had been established, the optimization process could give the optimum of the cycle parameters together with the selection of machines for a preliminary design. At the end of the process, the expander was identified as the critical CEG component because of the low inlet volumetric flow rate (315 g/s) which imposes a constraint to a full admission geometry. Furthermore, the high expansion ratio (about 3.32) and the low R404a sonic speed can lead to a supersonic flow inside the machine. Thus, the expander was design firstly. The selection of the basic commercial expander wheel has been carried on taking the transmitted torque into consideration. Once the proper shaft stem was selected, the corresponding expander wheel was fixed consequently, since turbochargers usually have the expander wheel welded with the shaft. In such a way, a Garrett wheel was selected and then modified reducing the blade height in order to address the proper expected fluid dynamic conditions. Moreover, the rotor was equipped with nozzle vanes to reach the expected velocities and flow angles at the rotor inlet [4, 8].

Some issues occurred for the preliminary design of the nozzle blades because the dynamic behaviour in transonic conditions of the working fluid R404a (a mixture of several fluids with different physical properties), is not well known. Thus, the preliminary geometry was modified replacing the first set of nozzle blades with a second one. Numerical results achieved using this new geometry are reported in [8 and 9].

Once the expander prototype design was ready, a suitable turbocharging compressor wheel was modified accordingly. In the next chapter, the numerical activities connected with the development of the first-generation CEG secondary compressor prototype are reported.

4. The secondary compressor

On the basis of the expander analysis, a secondary compressor power of 4.5 kW at 60000 rpm was taken into consideration for the nominal running point. A preliminary selection of an impeller commercially available has been conducted on the basis of the similarity rules described above. Then, for the nominal mass flow reported in Table I and fixing an expected compressor nominal efficiency of 0.75, a simplified 1-D analysis at the mean line has been carried out. R404a properties have been extracted from [10]. The compressor centrifugal impeller was reduced, cutting the channels in the outlet area, modifying it in a mixed-flow impeller in order to achieve the expected pressure ratio (about 1.6). In Figure 2a the modified impeller geometry is shown.

Moreover, the original compressor volute was replaced with a vaneless diffuser for the recovery of the outlet kinetic energy before the flow goes into a tank at the main compressor inlet. Furthermore, the machine should be equipped with an Inlet Guide Vane (IGV) to provide the better nominal inlet velocity direction at the nominal speed of 60000 rpm. In the present work, the numerical evaluations have been carried out using the simplified boundary condition of a uniform pre-swirl at the impeller inlet section. Authors are going to explore the interaction between IGV and impeller in a future design step.

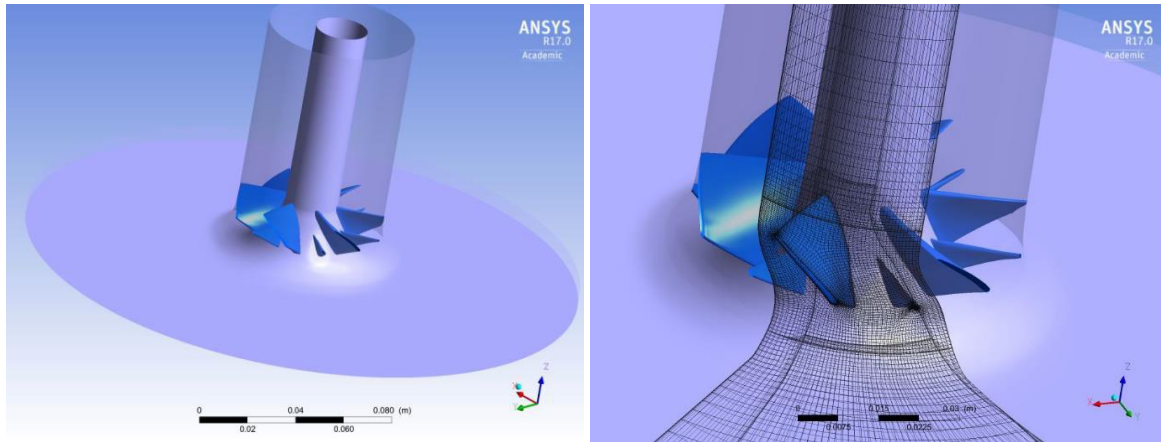


Fig. 2. (a) Secondary Compressor geometry; (b) 3D view of O-H grids for the rotor blades.

A O-H 3D computational mesh was generated for the simulation of two blade passages (figure 2b). The domain was extended beyond the impeller exit section to consider the vaneless diffuser. At the interface between the vaneless stator and rotor blades a frozen rotor interface was set. The frozen rotor approach is usually applied for preliminary design because it is able to give good prediction of overall performance characteristics in a fast way. Obviously, approximations connected with this approach (Coriolis and centrifugal forces added at the momentum equation) reduce simulations accuracy [11]. However, such a model was selected over more accurate ones, taking the design level of the present work into consideration.

Steady-state 3D viscous flow simulations were set up using a high-resolution advection scheme for the discretization of Navier-Stokes equations. In order to achieve preliminary information about the prototype capabilities, a standard SST $k-\omega$ model with scalable wall function was set up.

To describe the refrigerant, the real gas cubic equation Aungier Redlich Kwong Model was chosen [12]. Such a model provides a reasonable prediction of the real fluid behavior in the cases of interest. The model is based on the equation of state written as:

$$p = \frac{RT}{v-b+c} - \frac{a(T)}{v(v+b)} \quad (3)$$

$$a = a_0 \left(\frac{T}{T_c} \right)^{-n} \quad (4)$$

$$a_0 = \frac{0.42747 R^2 T_c^2}{p_c} \quad (5)$$

$$n = 0.4986 + 1.1735 \omega + 0.4754 \omega^2 \quad (6)$$

$$b = \frac{0.08664 R T_c}{p_c} \quad (7)$$

$$c = \frac{R T_c}{p_c + \frac{a_0}{v_c(v_c+b)}} + b - v_c \quad (8)$$

being ω , T_c and p_c the acentric factor and the critical temperature and critical pressure of the three pure R404a components (R125, R134a and R143a) respectively.

Four rotational speeds (from 40000 to 70000 rpm) have been considered. The total inlet pressure and temperature, the inlet velocity direction and the static pressure at the exit have been specified.

In Figures 3a and 3b performance characteristics related to the new prototype geometry (figure 2) are reported. In particular, figure 3a shows the pressure ratio versus the mass flow, while figure 3b shows the isentropic efficiency versus the mass flow. The isentropic efficiency is defined as:

$$\eta = \frac{h_{Tin} - h_{Tout}}{h_{Tin} - h_{Tisout}} \tag{9}$$

being h_{Tin} , h_{Tout} the total average enthalpies at the inlet and outlet section, respectively, and h_{Tisout} the isentropic total enthalpy at the outlet section of the entire machine.

In Figure 4a and b the static pressure ratio and the Mach number for the expected nominal running conditions (560 g/s and 60000 rpm) are presented.

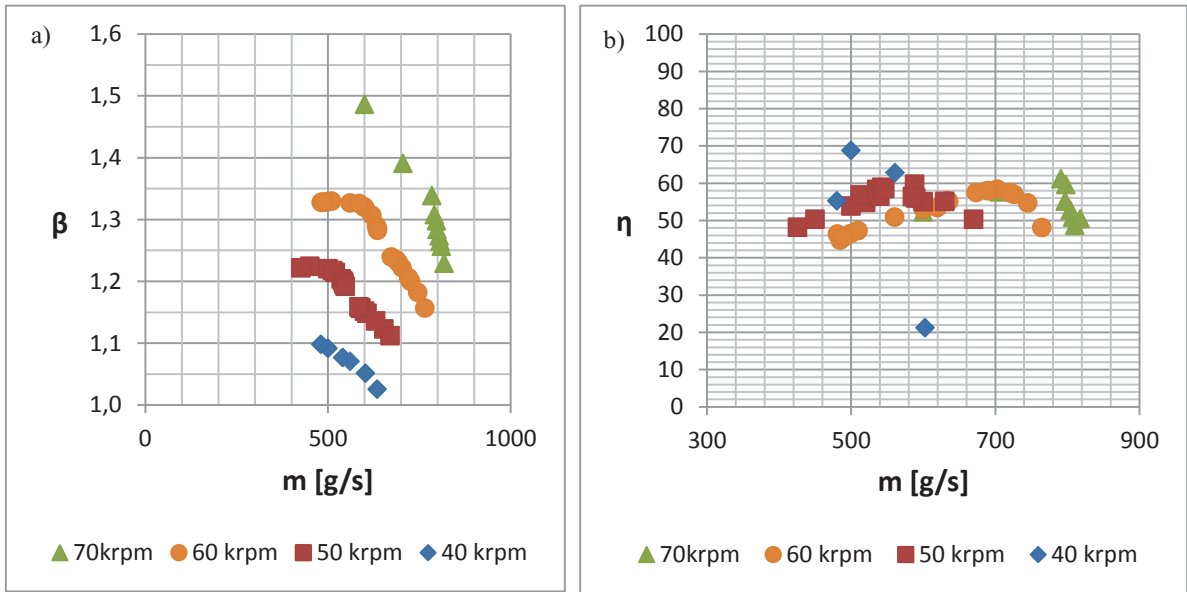


Fig. 3. Secondary compressor characteristics: (a) pressure ratio vs. mass flow; (b) isentropic efficiency vs. mass flow.

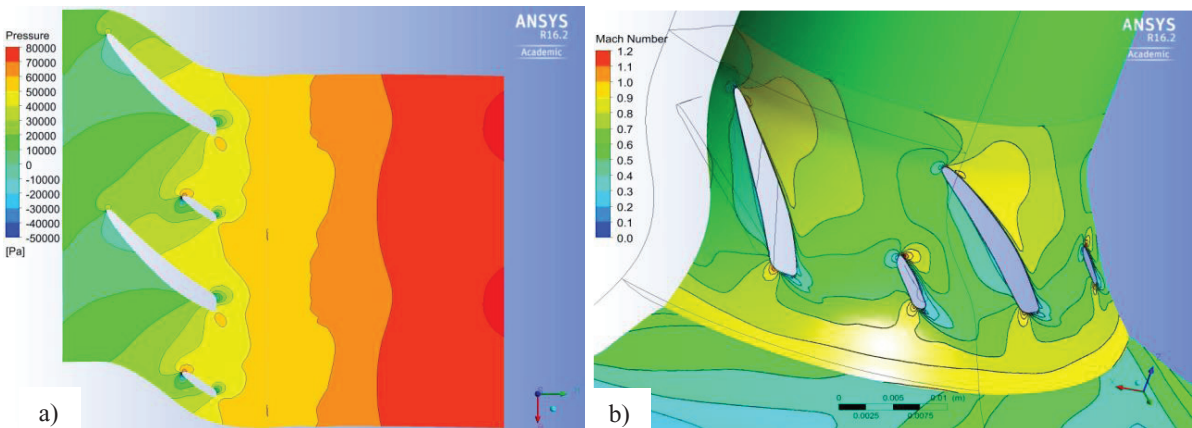


Fig.4. Nominal Running Point at mid-span: (a) static pressure contour; (b) Mach Number

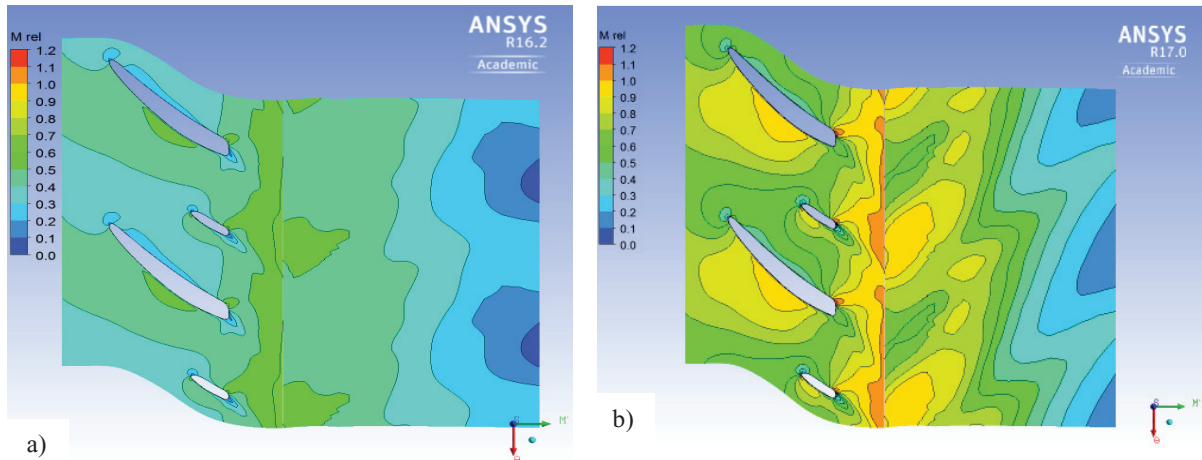


Fig. 5. Ma number at mid-span: (a) 40000 rpm, 540 g/s; (b) 70000 rpm 784 g/s.

They fit quite well with the results expected on the basis of the 1-D analysis. Nevertheless, the non-optimized blade and splitter shapes at the trailing edge and local high Mach numbers on the suction side and at the trailing edge reduce the machine potentialities. As shown in figure 3b the secondary compressor performance remains low at the nominal speed with an isentropic efficiency in the order of 55-60% except in the stall region where the efficiency drops down.

At off-design conditions, at lower speeds (40000 rpm), the compressible phenomena due to high local Mach numbers are less relevant and a peak in the isentropic efficiency can be detected. Such a peak is related to the condition of good coupling between the inlet relative velocity and the blade leading edge at constant pre-swirl angle given by the IGV. On the contrary, at higher speed the flow is partially choked at the impeller outlet section and wide transonic regions are detected inside the channels as depicted in Figure 5b.

5. Conclusions

This paper presents CFD modelling results for the performance evaluation of the first-generation secondary compressor prototype developed for an internal recovery system in VCR industrial plants.

The machine has been re-designed starting from a turbocharger compressor impeller available on the market. In order to address the new specifications, the outlet impeller section has been reduced, a swirl at the inlet section and a vaneless diffuser beyond the impeller outlet section have been added. Even if the impeller geometry has not been optimized, especially at the blade trailing edge, results are sufficiently in agreement with the expected performance. Some phenomena which reduce the machine performance are intrinsic factors, connected with the boundary conditions imposed by the plant (e.g. high Mach numbers at the nominal speed) and by the original geometry of the machines. Nonetheless, some specific aspects, like blade and splitter trailing edge shapes, can be modified improving the machine performance.

Therefore, the achieved results are a first positive response for the development of a secondary compressor for recovery systems in cryogenic plants.

Acknowledgements

Authors acknowledge the Italian Ministry for the Environment, Land and Sea, Angelantoni Industrie S.p.A., SETEL S.r.l. and Roma Tre University for their support to the COLD-ENERGY Project.

References

- [1] Confessore S., Development of an Expander-Compressor Group for energy saving in cooling systems, Master Thesis, Roma Tre University, 2010.
- [2] M. Ascani, Refrigerating Device and Method for Circulating a Refrigerating Fluid Associated With it, *United States Patent*; Patent No.: Us 8,505,317 B2; Aug.13, 2013.
- [3] Cerri G., Alavi S. B., Chennaoui L., Giovannelli A., Mazzoni S., Optimum turbomachine selection for power regeneration in vapor compression cool production plants, *International Journal of Mechanical, Aerospace, Industrial and Mechatronics Engineering* Vol. 9, No. 4, 2015.
- [4] Archilei E. M., Expander Compressor Group for energy saving in cryogenic plants, Master Thesis, Roma Tre University, 2012.
- [5] COLD-ENERGY Technical Report OR3-A3, Design, CEG prototype, Test bench, 2014.
- [6] S.L. Dixon, C.A. Hall, Fluid Mechanics and Thermodynamics of Turbomachinery, *Butterworth Heinemann*, Sixth Edition, 2010
- [7] O.E. Baljè, Turbomachines: A Guide to Design, Selection, and Theory, *John Wiley and Sons*, New York; 1980.
- [8] A. Giovannelli, E.M. Archilei, Design of an expander for internal power recovery in cryogenic cooling plants, *Energy Procedia*, Vol. 82; Dec 2015, pp. 180-185.
- [9] A. Giovannelli, E.M. Archilei, Internal Power Recovery in Cryogenic Cooling Plants. Part I: Expander Development, *International Science Index, Mechanical and Mechatronics Engineering*, Vol. 10, No. 6, 2016
- [10] NIST Reference Fluid Thermodynamic and Transport Properties – REFPROP Version 7.0.
- [11] A. Corsini, G. Delibra, A.G. Sheard, A critical review of computational methods and their application in industrial fan design, *Hindawi Publishing Corporation, ISRN Mechanical Engineering*, Vol. 2013, Article ID 625175.
- [12] Aungier R.H., A fast, accurate gas equation of state for fluid dynamic analysis applications, *Journal of Fluid Engineering*, Vol. 117, p. 277–281, 1995